Journal of Power Sources 196 (2011) 7957–7966

Contents lists available at ScienceDirect

Journal of Power Sources

journal homepage: www.elsevier.com/locate/jpowsour

Effect and siting of Nafion® in a Pt/C proton exchange membrane fuel cell catalyst

Jack Z. Zhang, Kitiya Hongsirikarn, James G. Goodwin Jr.*

Department of Chemical and Biomolecular Engineering, Clemson University, Clemson, SC 29634-0909, USA

ARTICLE INFO

Article history:
Received 17 March 2011
Received in revised form 13 May 2011
Accepted 19 May 2011
Available online 27 May 2011

Keywords:
H_2–D_2 exchange
Pt/C
Nafion-Pt/C
H_2 activation
PEMFC
Hydrogen surface concentration

ABSTRACT

This paper explores the effect and siting (location) of Nafion on Pt/C as exists in a PEM fuel cell catalyst layer. The addition of 30 wt% Nafion on Pt/C (Nfn-Pt/C) resulted in a severe loss of BET surface area by filling/blocking the smaller pore structures in the carbon support. Surprisingly, the presence of this much Nafion appeared to have only a minimal effect on the adsorption capability of either hydrogen or CO on Pt. However, the presence of Nafion doubled the amount of time required to purge most of the gas-phase and weakly-adsorbed hydrogen molecules away from the catalyst during hydrogen surface concentration measurements. This strongly chemisorbed surface hydrogen was determined by a H_2/D_2 switch and exchange procedure. Nafion had an even more pronounced effect on the reaction of a larger molecule like cyclopropane. Results from the modeling of cyclopropane hydrogenolysis in an idealized pores suggest that partial blockage of only the pore openings by the Nafion for the meso–macropores is sufficient to induce diffusion limitations on the reaction. The facts suggest that most of the Pt particles are in the meso–macropores of the C support, whereas Nafion is present primarily on the external surface of the C where it blocks significantly the micropores but only partially the meso–macropores.

1. Introduction

Proton exchange membrane fuel cells (PEMFCs) have been viewed by many as one of the most viable sources of clean energy available. Characteristics of PEMFCs, such as fast startup, high current density, and zero polluting emissions, render the technology ideal for automotive purposes [1].

Utilizing the redox reaction between hydrogen and oxygen to produce power, the general composition of a PEMFC consists of a proton transport membrane sandwiched in-between an anode and cathode catalyst layer. With the hydrogen oxidation reaction (HOR) occurring at the anode, oxygen reduction reaction (ORR) at the cathode, and the electrons produced conducted via an external circuit, fast transport of protons from the anode to the cathode depends almost entirely on the characteristics of the proton transport media utilized. For this purpose, most commercial PEMFCs favor a poly(perflourosulfonic acid) polymer, most commonly known as Nafion®, as the proton transport media due to their high proton conductivity, water uptake, and durability [2]. This Nafion constitutes the membrane as well as a part of the catalyst layers. In those layers it is present on the catalyst (typically Pt/C) in relatively large amounts (~30 wt%).

Before the protons produced from the HOR can reach the Nafion membrane, the activated hydrogen atoms must first be transported from the Pt site to a nearby Nafion cluster. This first transport step can take place either directly, if the Nafion is in direct contact with the Pt particle, or by diffusion on the carbon support. For this purpose, it is very advantageous to have high loadings of Nafion in the catalyst layer of a PEMFC to ensure fast transport of activated hydrogen atoms from the Pt to local Nafion clusters and then to the Nafion membrane. While high loadings of Nafion in the catalyst are important for fast proton transfer, one would hypothesize a negative effect of Nafion content on the activity of Pt for the HOR, i.e., by blocking Pt surface atoms via physical and/or chemical interactions, thereby preventing them from adsorbing and activating hydrogen.

To date, possible negative impacts of high loadings of Nafion on Pt activity for hydrogen activation have been studied via electrochemical techniques, such as cyclic voltammetry (CV) and rotating disk electrodes (RDE), and have only identified the large amounts of Nafion present to be effectively impeding HOR by obstructing the flow of feed gas and shifting the reaction from being kinetically controlled to being controlled by the diffusion of reactant gases to the catalysts [3–5]. While rate measurements were presented in these studies, due to the large amounts of Pt employed and the extremely fast reaction rate of HOR on Pt in the absence of any impurities, it is unclear whether the results can really be interpreted kinetically and were not affected by the H_2 activation reaction being at equilibrium. Furthermore, the electrodes used for the rotating disk voltammetry studies were immersed in a H_2-saturated solution, generally H_2SO_4,

* Corresponding author. Tel.: +1 864 656 6614; fax: +1 864 656 0784.
E-mail address: jgoodwi@clemson.edu (J.G. Goodwin Jr.).

0378-7753/$ – see front matter © 2011 Elsevier B.V. All rights reserved.
doi:10.1016/j.jpowsour.2011.05.052

with H_2-gas passing through the solution during the analysis. Such an environment may create adsorption/transport characteristics of the feed gas different than that in a fuel cell. Finally, high rotation speeds in the RDE exceeding 10,000 rpm have been known to create turbulence in the solution and cause unknown contributions of migration and cavitation effects [6]. These sources of extraneous error combined with a lack of adequate kinetic data demand a further look at whether the impregnation of such high weight loadings of Nafion on the catalyst particles in the catalyst layer of a PEMFC has an effect on the properties of Pt/C and in particular on the hydrogen activation capability of Pt.

As a continuation of our previous work, where the fundamental effects of CO poisoning on hydrogen activation on Pt/C catalysts were investigated utilizing the H_2–D_2 exchange reaction [7], research was carried out to investigate the interaction of Nafion on the properties of Pt in a commercial Pt/C catalyst commonly used in fuel cells. In addition to general catalyst characterization by BET, TEM, and static H_2/CO chemisorption, experiments were performed utilizing the H_2–D_2 exchange reaction for kinetic measurements of hydrogen activation in the presence of CO (a catalyst poison). In the absence of CO, the exchange reaction was at equilibrium and kinetic measurements could not be made. A modified H_2 to D_2 switch procedure, H_2–D_2 switch with Ar purge (HDSAP), was also used to measure in situ the surface concentrations of hydrogen and CO with time-on-stream (TOS). Furthermore, a structure sensitive reaction, cyclopropane hydrogenolysis, was employed as a characterization technique to magnify the obstructing effect, if any, of surface Pt sites by Nafion. All experimental results presented in this paper were obtained at conditions where reaction equilibrium was not a contributing factor. In addition, unlike the electrochemical studies, all reaction results were obtained for the catalysts exposed only to the gas-phase, where solution effects can be ignored.

2. Experimental

2.1. Catalyst preparation

A commercial Pt fuel cell catalyst, nominal 20 wt% Pt supported on carbon black (Pt/C), was purchased from BASF. It was confirmed by BASF that the carbon black support (Vulcan XC-72) was purchased in-bulk from Cabot Co. and used directly for the synthesis of the Pt/C catalyst.

Nafion supported on Pt/C (Nfn-Pt/C) catalysts were prepared via incipient wetness impregnation of the commercial 20 wt% Pt/C with a Nafion ionomer solution (LQ-1105, DuPont, 5 wt% Nafion) to give a target weight loading of 30 wt% for the Nafion. The 30 wt% loading of Nafion has been shown in the literature to be the optimum Nafion content in a PEMFC catalyst layer [8–11]. The impregnated material was dried at 90 °C overnight in a static air oven, crushed, and sieved to obtain a particle size of 60–150 μm. The catalyst was then stored in the dark prior to use. Nominal Pt composition was confirmed via elemental analysis (performed by Galbraith Laboratories) for both Pt/C and Nfn-Pt/C.

In order to verify all the possible sources of surface hydrogen in Nfn-Pt/C, to be discussed later, separate samples of Nfn-Pt/C were exchanged with either NaCl to neutralize the protonated sulfonic sites (SO_3^-–H^+) or exposed to 5000 ppm NH_3 gas to form (SO_3^-–NH_4^+). The Na^+-form of Nfn-Pt/C was prepared by ion-exchanging ca. 500 mg of Nfn-Pt/C with 30 mL of an aqueous solution of 0.1 M NaCl under constant agitation at room temperature for 2 days. The duration of the exchange process was adequate due to the solution containing only Na^+ ions. The exchanged sample was then filtered and rinsed 5 times with warm (70–80 °C) deionized water to remove excess solution. The resulting sample was dried overnight, crushed, sieved (60–150 μm), and kept in the dark prior to use. The NH_4^+-form of Nfn-Pt/C was obtained by exposing the catalyst to 5000 ppm NH_3 for 2 h after reduction in H_2 at 80 °C for 3 h. Due to the irreversible poisoning of Nafion by NH_3 [12], the high concentration of NH_3 was employed to ensure a fast and complete conversion of all available sulfonic sites to the ammonium form. As will be shown in Section 3.3, no effect on the surface hydrogen was observed from the treatment of Pt/C catalyst to NaCl and/or NH_3 gas using the same methodologies described.

2.2. Characterization methods

2.2.1. BET

BET surface area, pore size, and pore volume measurements were carried out with a Micromeritics ASAP 2020. Samples of Pt/C and Nfn-Pt/C were degassed under vacuum (10^{-3} mm Hg) at 110 °C for 4 h prior to analysis. Results were obtained from N_2 adsorption isotherms at −196 °C.

2.2.2. Static H_2/CO chemisorption

Chemisorption experiments using H_2 and CO were performed at 35 °C and 80 °C in a Micromeritics ASAP 2010 equipped with a chemisorption controller station. Due to the structural instability of Nafion at temperatures of 120 °C and above, catalysts were first reduced in H_2 at 80 °C for 3 h followed by an evacuation at 80 °C (10^{-5} mm Hg) for another 3 h prior to the start of the analysis. Temperature programmed reduction (TPR) results had shown the Pt to be fully reduced at these conditions. After evacuation, the temperature was then adjusted to the specified chemisorption temperature and the H_2 or CO isotherms were obtained from 50 to 450 mm Hg at increments of 50 mm Hg. Volumetric uptakes of CO or H_2 on the catalysts were determined from the total adsorption isotherm of the specified gas by extrapolating the higher pressure region of the total isotherm, which was linear, to zero pressure. These values were then used in determining total Pt surface atom concentration (Pt_S) and metal dispersion by assuming stoichiometric ratios of 1:1 for CO:Pt_S and H:Pt_S. Correlation with TEM has shown that this permits a reasonable estimation of metal particle size for Pt/C [7]. Calculation of average Pt particle size for Pt/C and Nfn-Pt/C were carried out using the metal dispersion calculated from the chemisorption results [7].

2.2.3. TEM and XRD

Transmission electron microscopy (TEM) images of Pt/C and Nfn-Pt/C were obtained using a TEM-Hitachi 9500, which offers 300 kV high magnification TEM and is designed for atomic resolution. Preparation of copper sample grids is explained in detail elsewhere [7]. Approximate Pt particle sizes of the catalysts were obtained by averaging diameters of 100+ particles from the TEM images. The results were further confirmed via X-ray Diffraction (XRD) (Scintag XDS 2000 powder diffractometer equipped with Cu Kα radiation) on as-received and reduced Pt/C and Nfn-Pt/C (80 °C in H_2 for 3 h) with a scanning range from 20° to 85° and a step-size of 0.02° min^{-1}.

2.2.4. Surface hydrogen concentration measurements

The method, H_2–D_2 switch with an Ar purge (HDSAP), was developed in our previous work [7] for determining in situ hydrogen surface concentration on Pt. The use of HDSAP is preferred over other surface concentration measurements, such as TPD, due to the non-destructive nature of the methodology and its ability to obtain TOS measurements. This is especially important for Nfn-Pt/C due to the thermal instability of the polymer at temperatures higher than 120 °C. Further explanation of the details and assumptions regarding HDSAP can be found elsewhere [7].

HDSAP measurements were initiated by flowing a gas mixture comprised of H_2/Ar (50:50) at 100 cm^3 min^{-1} (sccm) for 30 min (exposure phase). The H_2 was then turned off and 50 sccm of Ar was passed through the differential, plug flow reactor for 30 min or 50 min (purge phase) for Pt/C or Nfn-Pt/C, respectively. This was done to purge as much of the gas-phase or weakly adsorbed H_2 from the catalyst as possible. In the case of Nfn-Pt/C, a longer purge time was required due to the addition of high weight loadings of Nafion (see Section 3.3). After the purge phase, a flow of 50 sccm of D_2 (along with the 50 sccm of Ar) was introduced to the catalyst, resulting in two mass spectrometer signals being observed for hydrogen-containing species (H_2 and HD). The amount of H_2 and HD were calculated by integrating the area under the peaks (signal vs. time) and using the area obtained from a pulse of known quantities of H_2 and HD via a 6-port valve equipped with a 2 mL sample loop as calibration. Total surface concentration of hydrogen was calculated by adding the amount of hydrogen (H) in H_2 and HD, as given by the equation below:

$$\text{Surface H } (\mu\text{mol g.cat}^{-1}) = \mu\text{mol HD g.cat}^{-1} + 2 \times \mu\text{mol } H_2 \text{ g.cat}^{-1} \quad (1)$$

2.2.5. Cyclopropane hydrogenolysis

In order to better determine whether or not the high weight loading of Nafion was blocking surface Pt atoms via either physical and/or chemical interactions, a surface sensitive reaction, cyclopropane hydrogenolysis, was performed on 1 mg and 2.5 mg of Pt/C and Nfn-Pt/C, respectively, at 30 °C and 1 atm utilizing a conventional plug flow, micro-reactor system similar to the one described in reference [7]. The catalyst was diluted uniformly with 39 mg and 37.5 mg of XC-72 for Pt/C and Nfn-Pt/C, respectively, to achieve a catalyst bed of ca. 1 cm in thickness. Prior to reaction, catalysts were first reduced in 100 sccm of H_2/Ar (50:50) for 3 h at 80 °C and 1 atm, after which the temperature was decreased from 80 °C to 30 °C. Once the temperature was stable at 30 °C, reaction was initiated by flowing a gas mixture of C_3H_6:H_2:Ar (1:49:150) (total flow = 200 sccm) through the catalyst bed and allowing it to stabilize for 5 min before injecting the gas effluent into a Varian C gas chromatograph (GC) equipped with an FID detector for analysis. The FID was connected to a Restek RT-QPLOT column (30 m, 0.53 mm ID), capable of separating C_1–C_7 hydrocarbons. Due to the high activity of Pt for cyclopropane hydrogenolysis [13], low amounts of catalysts and a low partial pressure of C_3H_6 in the feed stream were required to achieve close to differential conditions for kinetic analysis. Variation of space velocities or particle sizes of the catalyst showed no change in reaction rate, indicating the lack of external and internal mass transfer effects, respectively. The apparent activation energy of cyclopropane hydrogenolysis on Pt/C from Arrhenius plots was found to be ca. 11.6 kcal mol^{-1}, which is well within the 8–12 kcal mol^{-1} range reported by Kahn et al. [14], and confirms, along with the linearity of the Arrhenius plot, the absence of mass or heat transfer effects on the rate of reaction measurements for Pt/C, the reference catalyst.

2.3. H_2–D_2 exchange reaction

The H_2–D_2 exchange reaction was chosen as the model reaction for the HOR primarily because both reactions share the same rate-limiting step, the dissociative adsorption of hydrogen. Furthermore, as shown by Ross and Stonehart [15], for the temperature range of 30–80 °C, the first-order rate constants for H_2–D_2 exchange on Pt and electrochemical hydrogen oxidation are in close agreement with each other. Thus, not only is the H_2–D_2 exchange reaction a good probe reaction for hydrogen activation, it is also a very good model reaction for the electrocatalytic oxidation of hydrogen on Pt, within the temperature range specified.

Using a conventional plug flow, micro-reactor system pressurized at 2 atm, the catalyst samples were pretreated at 80 °C in 100 sccm of H_2:Ar (50:50) gas mixture for 3 h. A detailed explanation and drawing of the experimental apparatus used for reactions involving H_2–D_2 exchange can be found elsewhere [7]. In order to keep the amount of Pt constant for comparison purposes, H_2–D_2 exchange rate measurements were obtained with catalyst samples of 5 mg Pt/C (having 17.5 wt% Pt) and 6.4 mg Nfn-Pt/C (having 13.7 wt% Pt) mixed with 35 mg and 33.6 mg of XC-72, respectively, to achieve a bed length of ca. 1 cm in thickness. Due to the high activity Pt exhibits for H_2–D_2 exchange, in addition to the low amounts of catalyst used, exposure of the catalysts to 30 ppm CO was done as a means to shift the exchange reaction away from equilibrium and into differential conversion as preferred for kinetic analysis.

After pretreatment, a gas mixture of H_2:Ar (50:50) containing 30 ppm CO was flowed over the catalyst at 80 °C for 12 h to achieve CO adsorption/desorption equilibrium such that no further change in HD signal was observed (steady-state). After achieving steady-state, measurements of the apparent activation energies (E_a) were started by flowing a reactant gas mixture at 80 °C and 2 atm comprised of H_2:D_2:Ar (25:25:50), still containing 30 ppm CO, over the catalyst for 15 min, with the effluent gas (comprised of the reactants H_2 and D_2, the product HD, and the inert Ar) being analyzed online with a Pfeiffer Vacuum mass spectrometer (MS). To obtain the MS signals of H_2 and D_2 in the absence of the catalyst for the purpose of calculating the exchange conversion, the flow was switched to reactor bypass for 5 min. The exchange conversion for H_2 or D_2 was obtained via Eq. (2) using the H_2 ($m/z = 2$) and D_2 ($m/z = 4$) MS signals in the presence and absence of catalyst:

$$\text{Conversion } (\%) = \frac{(H_2 \text{ or } D_2 \text{ signal})_{\text{No Cat.}} - (H_2 \text{ or } D_2 \text{ signal})_{\text{Cat.}}}{(H_2 \text{ or } D_2 \text{ signal})_{\text{No Cat.}}} \quad (2)$$

Under differential conditions, reaction rates were calculated by multiplying the measured conversion with the initial molar flow rate of hydrogen and dividing by the weight of Pt in the catalyst bed.

In order to determine the apparent activation energy, E_a, the temperature was then decreased to 70 °C, where the conversion was again obtained after reaching steady-state. This process was repeated for 60 °C, 50 °C, 90 °C, and finally at 80 °C again. The rate obtained at 80 °C at the beginning of the experiment was the same as the rate measured at 80 °C at the end of the experiment indicating that no deactivation occurred during the rate measurements. Similar to the cyclopropane hydrogenolysis experiments, variation of space velocities or particle size of catalyst showed no change in reaction rate, indicating the lack of external and internal mass transfer effects, respectively. The apparent activation energy of H_2–D_2 exchange on Pt/C, the reference catalyst, in the presence of CO from Arrhenius plots was found to be ca. 20 kcal mol^{-1}, the expected value [7], and confirms the absence of heat transfer effects on the rate of reaction measurements.

3. Results and discussion

3.1. Catalyst characterization

3.1.1. BET

BET surface area, pore size, and pore volume results for the carbon support (XC-72) were 225 m^2 g^{-1}, 16.4 nm, and 0.63 cm^3 g^{-1}, respectively, which correspond very well with literature values [16,17]. While the addition of Pt to the carbon support (performed by BASF) did little to affect the average pore size (15.9 nm), reduc-

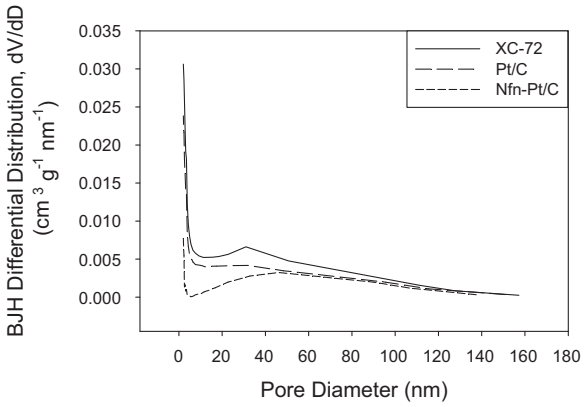

Fig. 1. Pore size distributions for XC-72, Pt/C, and Nfn-Pt/C.

tions in the BET surface area (to 170 $m^2\,g^{-1}$) and pore volume (to 0.44 $cm^3\,g^{-1}$) were observed. This indicates that significant amounts of the Pt particles were likely situated in the pore structure rather than the surface of the carbon support.

Impregnation of Pt/C with Nafion resulted in a reduction of BET surface area and pore volume from 170 $m^2\,g^{-1}$ and 0.44 $cm^3\,g^{-1}$ to 38 $m^2\,g^{-1}$ and 0.28 $cm^3\,g^{-1}$, respectively, while increasing the average pore size to 32.7 nm. Due to the fact that the majority of a support's surface area comes from its pore structure, this severe reduction in BET surface area suggests a filling/blocking of many of these pores by the Nafion, especially the smaller pores, while the slight reduction in pore volume suggests that the larger pores, which contribute most to pore volume were relatively open. Further analysis of pore size distribution for XC-72, Pt/C, and Nfn-Pt/C (Fig. 1), based on the desorption differential distribution calculated by the Barrett–Joyner–Halenda (BJH) method [18,19], confirms, more or less, a substantial filling/blocking of the smaller pores by Nafion while the larger sized pores appears to be less significantly blocked.

3.1.2. Elemental analysis

Elemental analysis results for Pt/C and Nfn-Pt/C from Galbraith Laboratories showed Pt loadings of 17.3 wt% and 13.7 wt%, respectively, and sulfur contents of 0.5 wt% and 1.2 wt%, respectively. The amount of sulfur obtained for Pt/C is similar to that of the carbon support (XC-72). While the residual sulfur (ca. 0.5 wt%) in the Pt/C is most likely due to the vulcanization process used in producing the activated carbon support, the additional sulfur obtained for Nfn-Pt/C (ca. 0.7 wt%) can be directly attributed to the sulfonic sites present in the polymer. Calculation of Nafion-loading based on the sulfur content shows a Nafion content of ca. 22 wt% and a sulfonic site concentration of ca. 231 μmol H^+–SO_3^- per g of Nfn-Pt/C or 1688 μmol H^+–SO_3^- per g of Pt. Using 1.58 g cm^{-3} as the approximate density of Nafion [20] and the BET surface area obtained for Pt/C (170 $m^2\,g^{-1}$), rough calculations suggest that there is enough Nafion in Nfn-Pt/C to produce an equivalent monolayer coverage of the catalyst at least 1.5 nm in thickness. Analysis of EDX mapping for Nfn-Pt/C showed the sulfur and fluorine contents to be evenly distributed on the surface of the catalyst.

3.1.3. Average particle size (TEM and XRD)

Analysis of TEM images indicated an even distribution of Pt particles on the carbon support (XC-72) for both Pt/C (Fig. 2a) and Nfn-Pt/C (Fig. 2b) catalysts. Average Pt particle sizes for the as-received Pt/C and the as-prepared Nfn-Pt/C were determined to be 2.6 ± 0.4 nm and 2.8 ± 0.5 nm, respectively, indicating no apparent change in Pt particle size (within experimental error) during Nafion loading. Exposure of Pt/C to H_2 and H_2/Ar at 80 °C for 24 h also had

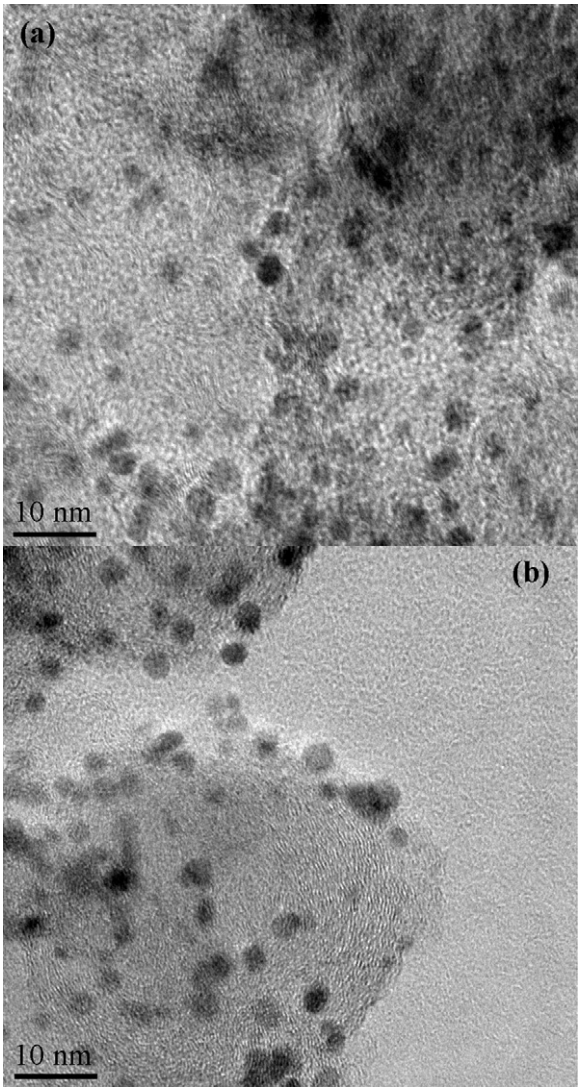

Fig. 2. TEM images of (a) Pt/C and (b) Nfn-Pt/C.

no effect on its average particle size (TEM results not shown), suggesting that the sintering process is extremely slow at 80 °C. Similar results were obtained via XRD using the Debye–Scherrer equation and the full width at half maximum (FWHM) of the Pt(1 1 1) diffraction peak for both Pt/C and Nfn-Pt/C (Fig. 3). Due to the rel-

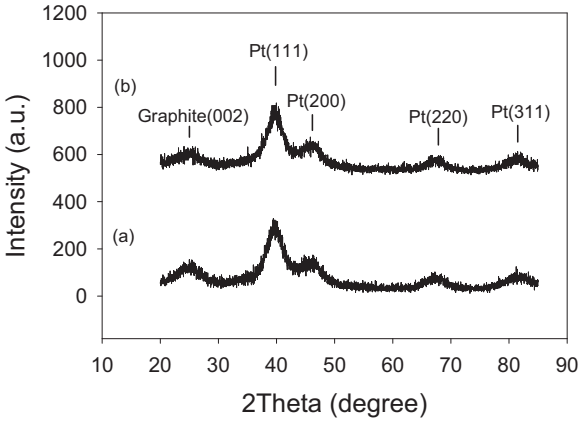

Fig. 3. XRD spectra of (a) Pt/C and (b) Nfn-Pt/C.

Table 1
Static H_2 and CO chemisorption results at 35 °C and 80 °C for Pt/C and Nfn-Pt/C.

Catalyst[a]	Adsorption gas	Analysis temp. (°C)	Amount of CO/H adsorbed[b] (μmol (g Pt)$^{-1}$)	Metal dispersion (%)	Avg. Pt particle size (nm)[c]
Pt/C	H_2	35	1806	35	3.1
		80	2063	40	2.7
	CO	35	1669	33	3.3
		80	1697	33	3.3
Nfn-Pt/C	H_2	35	1861	36	3.0
		80	2160	42	2.6
	CO	35	1452	28	3.9
		80	1452	28	3.9

[a] Catalysts were pretreated in H_2 at 80 °C for 3 h.
[b] Experimental error for all results was ca. ±5%.
[c] Avg. Pt particle size calculated from: Avg. Pt particle size (nm) = $\frac{1.08}{\text{metal dispersion}}$, assuming CO/$Pt_s$ = 1 and H/Pt_s = 1 [45].

atively small signal/noise ratio (S/N ∼ 4), average Pt particle sizes from the XRD spectra were able to be determined to be ca. 3 nm for both catalysts, similar to the TEM results considering the difficulty of detecting Pt particles <3 nm using Cu Kα radiation. The XRD spectra also illustrate the lack of difference in the crystalline structure of Pt between Pt/C and Nfn-Pt/C. From left to right, 2θ values of 25°, 40°, 46°, 68°, and 81° in Fig. 3 correspond to diffractions of graphite(0 0 2), Pt(1 1 1), Pt(2 0 0), Pt(2 2 0), and Pt(3 1 1), respectively [21,22]. Thus, results from both TEM and XRD appear to suggest an average Pt particle size of approximately 2.6–2.8 nm for both catalysts.

3.1.4. Static H_2 and CO chemisorption

Due to differing Pt loadings for Pt/C and Nfn-Pt/C, static chemisorption results were scaled to "per g of Pt" rather than "per g of catalyst" in order for a valid comparison. Similar to the static chemisorption results reported for Pt/C in our previous work [7], an increase in the amount of hydrogen uptake was observed for both Pt/C and Nfn-Pt/C when the analysis temperature was increased from 35 °C to 80 °C (Table 1), which can be directly attributed to hydrogen spillover onto the carbon support [22]. Surprisingly, the amounts of hydrogen uptake (on a Pt basis) for both Pt/C and Nfn-Pt/C were identical, within experimental error. Even the effect of analysis temperature on hydrogen spillover was roughly the same for both catalysts, suggesting that Nafion did not inhibit the hydrogen adsorption capability of Pt through either physical blocking or chemical interactions, even though such a large amount of Nafion was present. While some of the Pt may exist in the smaller sized pores of the carbon support, based on the severe loss of pores with pore sizes of 20 nm and below between Nfn-Pt/C and Pt/C (Fig. 1) and the lack of an inhibition effect by the Nafion for the adsorption of H_2 mentioned above, it can be speculated that the majority of the Pt particles are most likely not in the smaller sized pores (≤20 nm).

As expected, an increase in the analysis temperature had no effect on the amount of CO uptake because CO does not spill over onto the carbon support at these temperatures. However, lower amounts of CO uptake than hydrogen (in atoms) were observed for the same catalyst. For Pt/C, the difference between hydrogen and CO uptake can be explained by the existence of both linear and bridge-bonded CO on Pt, as shown by DRIFTS results in our previous work [7], such that the overall stoichiometry of CO:Pt_S is actually less than 1. The addition of Nafion to Pt/C resulted in a somewhat lower CO uptake than for Pt/C alone. While it may have been possible that the presence of Nafion has an effect on the interaction of CO with Pt such that the amount of linear and bridge-bonded CO on Pt for Nfn-Pt/C was different than that for Pt/C, due to the partial blocking of pores by the Nafion, evidenced by the pore size distribution (Fig. 1), and the similarity between critical diameters of N_2 and CO (3.0 Å vs. 2.8 Å, respectively), the difference in CO uptake between Pt/C and Nfn-Pt/C may more likely to have been due to Nafion preventing CO from reaching some of the Pt surface. This blockage may not have been observed for hydrogen perhaps because the critical diameter, defined as the "diameter of a cylinder which can circumscribe the molecule in its most favorable equilibrium conformation" [23], for hydrogen is 2.4 Å whereas the critical diameter for CO is 2.8 Å. Thus, the larger sized CO molecule may have been obstructed by Nafion from reaching Pt particle surfaces in places where the smaller sized hydrogen molecule would have no problem. Based on the significant reduction in BET surface area from Pt/C to Nfn-Pt/C and the fact that N_2 molecules have a critical diameter of 3.0 Å, similar to that of CO, a comparable reduction in CO uptake should have occurred for Nfn-Pt/C if Pt particles were evenly distributed in the pore structure of the carbon support. However, the actual slight reduction in CO uptake for Nfn-Pt/C reaffirms the earlier hypothesis that the majority of the Pt particles are most likely not situated in the smaller pores (≤20 nm) of the carbon structure. In other words, the smaller Nafion-filled/blocked pores that blocked N_2 molecules from getting through also blocked CO molecules; however, because there were probably few or no Pt particles in those smaller pores, the amount of CO uptake measured by static chemisorption was not significantly reduced.

It should be noted that the physical characteristics of a catalyst can vary depending on the precursor used, method of preparation, treatment conditions, type of support, etc. For example, pore volume distributions of various carbon supports prepared via the oil-furnace or acetylene process [24] show that the majority of the pore diameters were less than 10 nm. The reason for such small pore diameters is most likely due to the fact that the carbon particles themselves ranged from 10 to 40 nm in diameter, whereas the size of carbon particles used in this study were ca. 60–150 μm in diameter. Thus, when comparing the physical characteristics between catalysts, all variables, such as the ones mentioned above, must be taken into consideration.

3.2. H_2–D_2 exchange reaction

Apparent activation energy (E_a) measurements for H_2–D_2 exchange reaction on Pt cannot be obtained in the absence of a catalyst poison due to the reaction being limited by equilibrium at the experimental conditions used in this study, even for very small quantities of catalysts. Therefore, prior to the gathering of kinetic data, catalysts were exposed to 30 ppm of CO to partially cover the Pt surface ($\theta_{CO} \approx 0.71$ monolayer) and to shift the reaction away from equilibrium. All results reported in this section were obtained after the adsorption–desorption of CO had reached steady-state.

Similar to the results presented in our previous study [7], exposure of Pt/C to the CO resulted in an apparent E_a of 20.3 ± 0.5 kcal mol^{-1} for the poisoned Pt surface compared to an apparent E_a of 4.5–5.4 kcal mol^{-1} reported for an unpoisoned Pt surface [21,25]. Similarly, exposure of Nfn-Pt/C to 30 ppm CO resulted in an apparent E_a of ca. 21.5 ± 1.0 kcal mol^{-1}. No difference was observed in the rate of HD formation from H_2–D_2

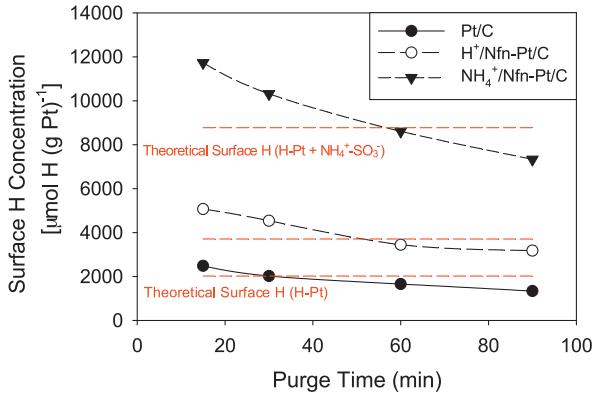

Fig. 4. Effect of purge time on hydrogen surface concentration measurements on Pt/C, Nfn-Pt/C, and the NH_4^+ form of Nfn-Pt/C.

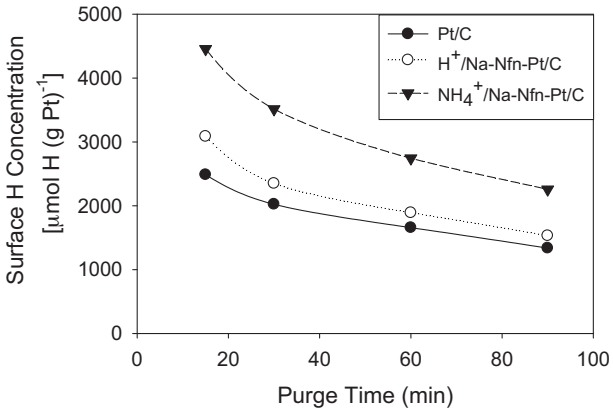

Fig. 5. Effect of sulfonic sites exchanged with Na^+ ions on hydrogen surface concentration on Nfn-Pt/C.

exchange for Pt/C [1080 ± 50 μmol HD (g Pt)$^{-1}$ s^{-1}] and Nfn-Pt/C [1065 ± 63 μmol HD (g Pt)$^{-1}$ s^{-1}], both in the presence of 30 ppm CO. This similarity in both apparent activation energy and reaction rate between the two catalysts reaffirms that the Pt particles are most likely in the larger pore structures of the carbon support and that the Nafion does not appear to be inhibiting the adsorption of either hydrogen or CO on the Pt surface via any physical and/or chemical interactions.

3.3. *In situ TOS surface hydrogen concentration via HDSAP*

Due to the extremely fast reaction rate of H_2–D_2 exchange in the presence of Pt, any amount of hydrogen trapped either in the pores of the support or in the Nafion clusters at the onset of the D_2 switch during HDSAP would cause an overestimation in the hydrogen surface concentration measurement. Thus, while a purge time of 30 min was enough to remove most of the excess hydrogen trapped in the pores of Pt/C [7], the same amount of time might not be sufficient due to the presence of Nafion on the catalyst.

Fig. 4 shows the amount of hydrogen surface concentration as a function of purge time used for HDSAP measurements. Total surface concentration of hydrogen was calculated via Eq. (1) by measuring the amount of HD and H_2 formed at the onset of the D_2 switch. As can be observed from the figure, a 30 min purge time with Ar for Pt/C, prior to the introduction of D_2, yields a hydrogen surface concentration similar to that from static hydrogen chemisorption on Pt/C at 80 °C. This result suggests that for Pt/C, a purge time of 30 min is sufficient to remove most of the excess hydrogen in the pores of Pt/C without affecting the strongly adsorbed hydrogen associated with Pt (H-Pt). However, in order for the hydrogen surface concentration for Nfn-Pt/C to be similar to the theoretical total amount of exchangeable surface H, which is the sum of static hydrogen chemisorption at 80 °C [H-Pt ≈ 2160 μmol H (g Pt)$^{-1}$] and the concentration of sulfonic sites in the Nafion [SO_3^-–H^+ ≈ 1688 μmol H (g Pt)$^{-1}$], a purge time of 50 min is required. This increase in purge time required was also observed for samples of Nfn-Pt/C exposed to NH_3 (gas), which increased the amount of exchangeable surface hydrogen from Nafion from 1 hydrogen atom per sulfonic site to 4 hydrogen atoms due to the formation of SO_3^-–NH_4^+. In contrast, exposure of Pt/C to NH_3 (gas) prior to HDSAP showed a negligible effect on the surface hydrogen concentration. A likely reason for the difference in HDSAP purge times required between Pt/C and Nfn-Pt/C may be due to the Nafion clusters acting as a barrier to the diffusion of gas-phase H_2 away from the catalyst, as suggested earlier. Thus, a purge time of 50 min was chosen for surface hydrogen measurements for Nfn-Pt/C. Increase in purge time appeared to have a negligible effect on the removal of H^+ from the sulfonic sites during the Ar purge.

In order to verify whether the excess hydrogen is indeed from the sulfonic sites in the Nafion, separate samples of Nfn-Pt/C were poisoned by ion-exchanging the H^+ cations with a non-proton containing cation, Na^+. From these results, poisoning of sulfonic sites with Na^+ cations (Fig. 5) significantly decreased the hydrogen surface concentration from Na^+-Nfn-Pt/C compared to Nfn-Pt/C, giving values close to those of Pt/C. The slightly higher surface hydrogen concentration found for Na^+-Nfn-Pt/C than for Pt/C is due to a portion of the sulfonic sites being not fully exchanged with Na^+ but still being in the protonated form (H^+/Na^+-Nfn-Pt/C). Exposure of H^+/Na^+-Nfn-Pt/C to NH_3 (gas) resulted in the conversion of just the protonated sulfonic sites to the ammonium form (NH_4^+/Na^+-Nfn-Pt/C); calculations from the results suggest that ca. 4.5 out of 5.5 sulfonic sites had been poisoned with Na^+. The Pt/C catalyst treated with NaCl in an identical fashion yielded surface hydrogen concentration results similar to those of untreated Pt/C, which confirmed that the Na^+ was associated only with the Nafion. The poisoning results involving NH_3 and Na^+ clearly show the excess surface hydrogen concentration measured for H^+/Nfn-Pt/C to be from the protonated sulfonic sites in the Nafion. In addition, these results also confirm the rapid transport of protons from the surface Pt atoms to nearby Nafion clusters and vice versa, which is the desired intent of having such a high weight loading of Nafion. Thus, contrary to the previous idea that contact must be maintained between the Pt particles and the polymer electrolyte in order for proton transport to take place [24,26], surface diffusion of protons on the carbon support, while slower than on Pt [27], appears to be adequate for the reaction. The poisoning of the sulfonic sites by NH_3 did not appear to have an effect on this transport process (where D exchanges with NH_4^+).

3.4. *Effect of Nafion on the surface coverage of ppm CO in H_2 on Pt*

Possible effects of Nafion on the surface coverage of CO on Pt from ppm quantities of CO in H_2 were investigated indirectly via hydrogen surface concentration measurements. Similar to the CO surface coverage experiments performed on Pt/C in our previous work [7], TOS measurements of hydrogen surface concentration were measured for both Pt/C and Nfn-Pt/C over a 24 h period of exposure to 30 ppm CO in H_2.

The poisoning behavior of 30 ppm CO on Pt/C in terms of surface hydrogen concentration was analogous to the results presented in our previous study [7]. Surface coverage of Pt by CO for the Pt/C catalyst here was calculated to be ca. 0.71 monolayer (ML). The difference between the CO surface coverage of 0.71 ML measured for the current batch of Pt/C and the 0.54 ML for the batch used in our previous study under identical conditions were likely due

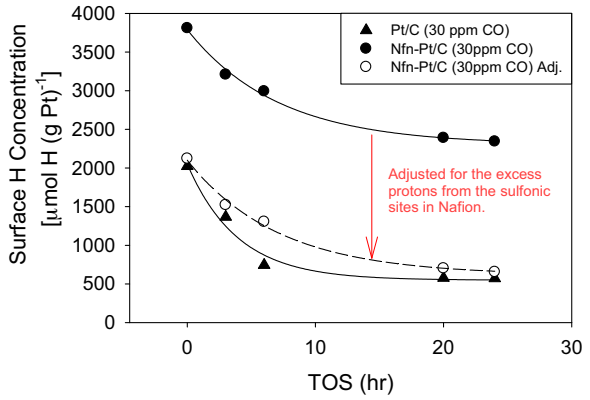

Fig. 6. Effect of Nafion on the surface coverage of CO on Pt/C and Nfn-Pt/C from 30 ppm of CO in H_2.

to slight differences in the preparation method by BASF for the different batches of Pt/C, thus changing the innate properties of the catalyst somewhat. Regardless, the measured CO surface coverage of 0.71 ML is similar to the 0.5–0.7 ML coverage range of CO observed on Pt(1 1 1) over the pressure range (P_{CO}) of 10^{-6} to 760 Torr at room temperature found via high pressure scanning tunneling microscopy (HP STM) and confirmed with calculations using density functional theory (DFT) [28–30].

From Fig. 6, the poisoning behavior of 30 ppm CO on Nfn-Pt/C, after adjusting for the excess surface hydrogen from the sulfonic sites in Nafion, is similar to that for Pt/C. The hydrogen surface concentration for Nfn-Pt/C, after 24 h of exposure to 30 ppm of CO, was somewhat higher than that for Pt/C, 660 μmol H (g Pt)$^{-1}$ vs. 570 μmol H (g Pt)$^{-1}$, respectively. Upon closer inspection, it can be observed that the addition of Nafion resulted in an apparent slightly slower approach to steady-state than for Pt/C at the same concentration of CO, which may account for the difference in the surface hydrogen measured. While this may be argued to be related to the longer purge time required for HDSAP measurements for Nfn-Pt/C versus for Pt/C, the more likely possibility is that of the large Nafion clusters interfering with the rate at which CO reaches the surface Pt atoms as it was confirmed that the increase in required purge time between Pt/C and Nfn-Pt/C did not have an effect on the surface coverage of strongly-bound CO. Thus, the hydrogen surface concentration for Nfn-Pt/C was most likely not at steady-state at 24 h, and further exposure of Nfn-Pt/C to CO would have resulted in a hydrogen surface concentration even more similar to that of Pt/C. Regardless, the CO surface coverage for Nfn-Pt/C and for Pt/C after 24 h of exposure is the same (0.69 vs. 0.71, respectively), within experimental error. The CO surface coverage results show that the Nafion does not, in general, appear to affect significantly the adsorption of CO on Pt at steady state. Similar to effect Nafion has on the rate of diffusion of CO, the slightly lower CO uptake observed for Nfn-Pt/C, compared to Pt/C, from static chemisorption results is mostly likely due to the system not being perfectly at equilibrium (i.e., the equilibration interval was too low for Nfn-Pt/C).

3.5. Effect of Nafion on the activity of Pt/C for cyclopropane hydrogenolysis

Up until this point, the presence of such a high weight loading of Nafion has appeared to have a lack of effect on the activity of Pt for the adsorption of hydrogen and CO, which is extremely surprising considering the significant reduction in BET surface area from the impregnation of the Nafion and the large amount of Nafion present. Even if the majority of the surface Pt resided in the larger pore structures of the carbon support, one would think that the presence of such a large amount of Nafion would have at least some effect on the Pt via physical and/or chemical interactions. Because the results given so far have all involved the activation of hydrogen in one form or another, this apparent lack of effect from the Nafion may be due to the fast kinetics of hydrogen diffusion and activation and the structure insensitive characteristic of activation. To probe this issue further, a more structure sensitive reaction was employed to provide further insight. Use of a "demanding" or "structure sensitive" reaction is often very useful for investigating metal dispersion and metal decoration effects on specific activity in heterogeneous catalysts [31]. One should understand that the term "structure sensitivity" entails not just an effect of metal particle size on the observed rate or turn-over-frequency of the reaction; rather the reaction rate of a structure sensitive reaction depends on the coordination number of the active metal surface atoms and/or the number of contiguous metal surface atoms (site ensemble size) required for reaction to occur. Thus, as the name implies, these structure sensitive reactions are sensitive to changes in the surface structure of the catalyst and the availability of the surface atoms.

For this study, the hydrogenolysis of cyclopropane was chosen as a structure sensitive reaction mainly due to its lower reaction temperature requirement for Pt-based catalysts (0–80 °C [32]). Other structure sensitive reactions, such as ethane hydrogenolysis, require operating temperatures in excess of 300 °C and above [33,34], which is problematic for the catalysts employed due to Nafion degradation at temperatures above 120 °C. In addition, at temperatures below 150 °C, only one product (propane) is formed from the reaction of cyclopropane with hydrogen over Pt catalysts, which greatly simplifies analysis [14,35]. While there exists differing opinions as to whether hydrogenolysis of cyclopropane over Pt catalysts is structure sensitive [13,36,37] or structure insensitive [14,35,38,39], results from a recent investigation [40] using K^+-modified Pt/C catalysts confirm the reaction to be structure sensitive.

Reaction rate measurements were obtained using small amounts of catalyst (1.0–2.5 mg), low reaction temperature (30 °C), and low concentration of reactants (0.05 atm C_3H_6 and 0.25 atm H_2), to ensure differential reaction conditions. In order to compare the rates, given the different wt% of Pt before and after loading Nafion, rates were calculated on a per weight Pt basis. Observed rates were calculated to be 557 μmol C_3H_8 (g Pt)$^{-1}$ s^{-1} and 373 μmol C_3H_8 (g Pt)$^{-1}$ s^{-1} for Pt/C and Nfn-Pt/C, respectively. Furthermore, determination of E_a from Arrhenius plots show the value for Nfn-Pt/C (5.4 kcal mol^{-1}) to be almost exactly half that of Pt/C (11.6 kcal mol^{-1}). This difference in E_a, where the measured (Nfn-Pt/C) is ca. half that of the intrinsic (Pt/C), is a very strong indication for the possibility of internal diffusion limitations, such that the reaction rate is shifted from being reaction-limited to diffusion-limited. Because E_a is an average value, interactions between Nafion and Pt, such as preferential blocking of specific Pt surface atoms and/or electronic effects where the surface binding energies of species are different, may also have a similar effect in shifting the value of E_a measured. However, since there exists no evidence thus far from all previous results suggesting that such an interaction exists, especially to the degree of reducing the values of E_a (measured for Pt/C) by half, the possibility of internal diffusion limitations caused by the Nafion will be discussed.

In this case, because no signs of internal diffusion limitations are evident for Pt/C, it can only be concluded that the presence of internal diffusion limitations observed for Nfn-Pt/C is due to the Nafion. Based on previously mentioned evidence suggesting that the majority of the Pt appears to be in the larger pore structures (>30 nm) of the carbon support and the lack of evidence suggesting the filling of these pores by the Nafion (i.e., only a subtle decrease in pore size distribution based on pore volume, Fig. 1), it can be proposed that the main cause of internal diffusion limitations observed for Nfn-Pt/C is probably due to the partial blocking of pore openings

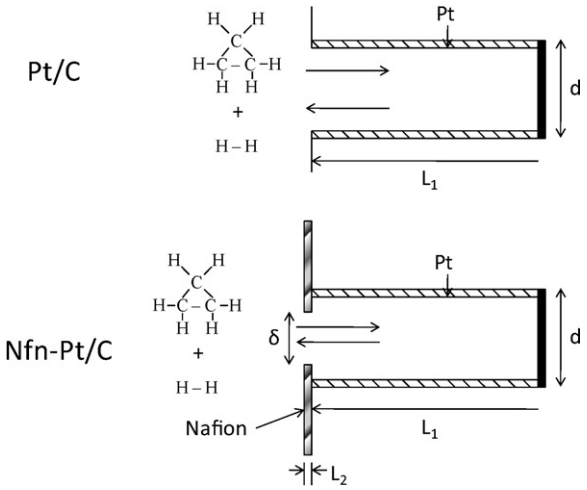

Fig. 7. Simplified scenario of blocking of pore opening by the Nafion in Nfn-Pt/C.

by the polymer, such that the diameter of the entrance into a pore (δ) is smaller than the diameter of the pore (d) itself (as illustrated in Fig. 7).

Theoretical modeling of the effect of δ on the E_a was performed using a single one-dimensional ideal cylindrical pore with a length of L_1 and a diameter of d; factors such as tortuosity, pore porosity, and constriction factor were all assumed to be unity. Using a similar scenario depicted by El-Kady and Mann [41] in their work regarding the deactivation of catalyst due to pore-mouth plugging from coke deposition, the Nafion was assumed to form a membrane as an impenetrable barrier of thickness L_2 with an opening to the pore of diameter δ. Assuming a first-order irreversible reaction, which is a reasonable assumption for cyclopropane hydrogenolysis in the presence of a large excess of hydrogen [32], at steady-state, the mass-balance (in dimensionless form) for species A in the system is (Eqs. (3) and (4)):

$$\text{In membrane}: \quad \frac{d^2C_2}{d\eta^2} = 0 \tag{3}$$

$$\text{In the pore}: \quad \frac{d^2C_1}{d\eta^2} - \left(\frac{4kL^2}{dD_{e,1}}\right) C_1 = 0 \tag{4}$$

with the following dimensionless variables:

$$\eta = \frac{x}{L}, \qquad C_1 = \frac{C_{A,1}}{C_{A,o}}, \qquad C_2 = \frac{C_{A,2}}{C_{A,o}} \tag{5}$$

These conservation of mass equations are derived based on Fick's law for dilute solutions and can be found in any transport-related textbook [42]. The variable L is the total length of the system and is the sum of L_1 and L_2, $C_{A,o}$ is the bulk concentration of species A outside of the pore, $D_{e,1}$ is the effective diffusivity inside the pore, $C_{A,1}$ and $C_{A,2}$ are the concentration of species A in the pore and membrane, respectively. Boundary conditions used to solve the above differential equations are:

$$\text{At} \quad \eta = 0 \quad (\text{end of the pore}): \quad \frac{dC_1}{d\eta} = 0 \tag{6}$$

$$\text{At } \eta = 1: \quad C_2 = \Phi_2 \tag{7}$$

$$\text{At } \eta = \frac{L_1}{L} = \lambda_1 \text{ (interface between membrane and pore)}:$$

$$\Phi C_1 = C_2, \quad \text{where } \Phi = \frac{\Phi_2}{\Phi_1} \tag{8}$$

$$\text{At } \eta = \frac{L_1}{L} = \lambda_1: \quad D\frac{dC_1}{d\eta} = \frac{dC_2}{d\eta}, \quad \text{where } D = \frac{D_{e,1}}{D_{e,2}} \tag{9}$$

where $D_{e,2}$ is the effective diffusivity in the membrane, Φ_1 and Φ_2 are the partition coefficients for the pore and membrane respectively. The partition coefficient Φ is the ratio of available volume to the void volume and is dependent on the molecular properties of the solute. So, for cyclopropane, which has a critical diameter of ca. 4.9 Å or 0.49 nm, the partition coefficients for the membrane and pore are calculated by:

$$\text{Membrane}: \quad \Phi_1 = \left(1 - \frac{0.49\,\text{nm}}{\delta}\right)^2 \tag{10}$$

$$\text{Pore}: \quad \Phi_2 = \left(1 - \frac{0.49\,\text{nm}}{d}\right)^2 \tag{11}$$

The effective diffusivities $D_{e,1}$ and $D_{e,2}$ are defined as:

$$D_{e,1} = \frac{\varepsilon_1\sigma_1 D_{K,1}}{\tau_1} \quad \text{and} \quad D_{e,2} = \frac{\varepsilon_2\sigma_2 D_{K,2}}{\tau_2} \tag{12}$$

For both pore and membrane, the parameters: constriction factor (σ) and tortuosity (τ) are all assumed to be unity. The porosity for the ideal pore (ε_1) is also assumed to be unity while the porosity for the membrane (ε_2) is the ratio of the open area to the total area of the pore. The terms $D_{K,1}$ and $D_{K,2}$ are the Knudsen diffusion coefficients for the pore and membrane, respectively, and were calculated as follows:

$$D_{K,1} = \frac{d}{3}\sqrt{\frac{8RT}{\pi M}} \quad \text{and} \quad D_{K,2} = \frac{\delta}{3}\sqrt{\frac{8RT}{\pi M}} \tag{13}$$

where R is the gas constant, T is temperature, and M is the molecular weight of the solute. Solving for C_2 and C_1 from the differential Eqs. (3) and (4) via the boundary conditions Eqs. (6)–(9) yields the following solutions:

$$\text{In the membrane}: \quad C_2 = \Phi_2 - \alpha_2(1 - \eta) \tag{14}$$

$$\text{In the pore}: \quad C_1 = \alpha_1 \cosh(\phi\eta) \tag{15}$$

where

$$\alpha_1 = \frac{\Phi_2}{\Phi\cosh(\phi\lambda_1) + D\phi\sinh(\phi\lambda_1)(1 - \lambda_1)} \tag{16}$$

$$\alpha_2 = D\alpha_1\phi\ \sinh(\phi\lambda_1) \tag{17}$$

$$\phi = L\sqrt{\frac{4k}{dD_{e,1}}} \tag{18}$$

Approximation of average pore radius and pore length based on BET surface area, pore volume, gross volume of catalyst particle, and external surface area obtained for Pt/C show values of ca. 5 nm and 20 μm, respectively. The Arrhenius plot of the rate resulting from the concentration in the pore (C_1) is plotted in Fig. 8 with varying values for the diameter of the opening in the membrane.

It can be observed from Fig. 8 that in the case where opening in the membrane is equal to pore diameter (i.e., $\delta = d = 10$ nm), the theoretical E_a is the intrinsic value and no evidence of internal diffusion limitations exists. As the value of δ decreases, the concentration in the pore (C_1) and the resulting E_a does not start to be affected until δ is as low as 0.7 nm. Further decreases in δ beyond that point shifts the theoretical E_a farther from its intrinsic value of 11.5 kcal mol^{-1}, until finally, at a value of 0.5 nm, the δ was so small that almost no solute, in this case cyclopropane with a critical diameter of ca. 0.49 nm, is able to diffuse into the pore, thus yielding an E_a close to zero. It should be noted that for all values of δ, the concentration gradient, at steady-state, remained relatively constant throughout the pore. Even at a δ value of 0.55 nm, where the E_a showed clear diffusion limitations, the steady-state concentration of cyclopropane

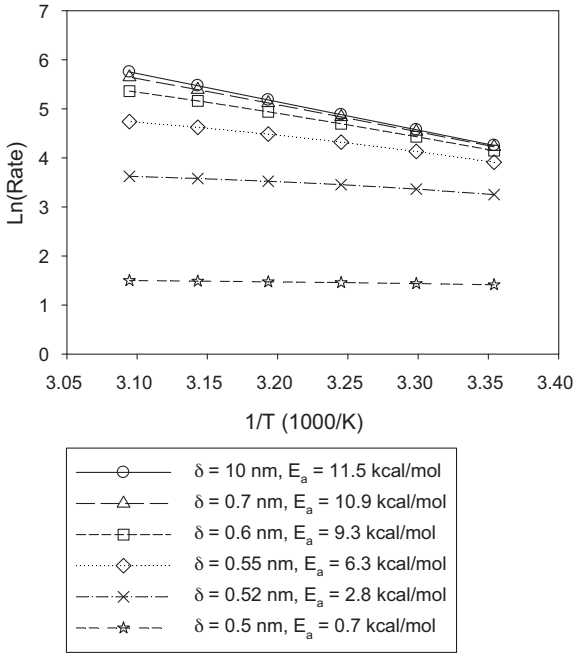

Fig. 8. Effect of membrane opening on E_a for cyclopropane hydrogenolysis on Pt/C using an idealized cylindrical pore model with the pore mouth partially covered by a (Nafion) membrane.

in the pore was ca. a factor 0.6 that of the bulk and varied no more than 0.02% from one end of the pore to the other. This lack of a concentration gradient in the pore is counterintuitive for a supposedly diffusion-influenced reaction. But this is just because most people are used to the effect of decreasing diameter of the pore. The real diffusion barrier is the membrane in the current case. It is important to note that the model is based upon a simple mass-balance and does not take into account wall effects and other electronic interactions on diffusion. In the presence of these effects, the effect of membrane diameter may be even larger.

Increases in the number of openings in the membrane also increase the calculated E_a for the same opening diameter. For example, if there exists 5 openings in the membrane each with $\delta = 0.55$ nm, the calculated E_a would increase from 6.3 kcal mol^{-1} (only 1 opening) to 9.8 kcal mol^{-1} and the calculated E_a for $\delta = 0.52$ nm would increase from 2.8 kcal mol^{-1} to 6.8 kcal mol^{-1}. However, because the model does not take into account wall effects and other electronic interactions, no definite conclusions can be made regarding this change.

Attempts were made to obtain actual cross-sectional spectra of a Nfn-Pt/C catalyst particle via both SEM/EDX and TEM/EDX by imbedding the catalyst particles in a resin. The dried resin was then either cut/polished for SEM/EDX analysis or sectioned via microtone for TEM/EDX analysis. Results from both methods proved to be inconclusive due mostly to the lack of penetration of the resin into the carbon support. The fragile nature of the carbon also proved to be troublesome.

Based on these and all previous results, it can be concluded that the effect of Nafion on Pt/C for cyclopropane hydrogenolysis appears to be limited to the induction of internal diffusion limitations by virtue of decreasing the effective diameter of the openings of the pores in the carbon support. The similar values of E_a observed for H_2–D_2 exchange reaction on both catalysts, poisoned with ppm CO, suggests that either the openings of the pores or the openings in the Nafion structure itself overlaying the pores were wide enough so that hydrogen diffusion was not affected. No blocking of Pt surface atoms by the Nafion via either physical and/or chemical interactions was observed. It is important to note that while the Nafion in this study was in the dry or unswelled state. Due to the apparent lack of interactions between the polymer and Pt surface and the minimal impact water vapor has for H_2 adsorption and activation on Pt/C [43], the effect that humidity would have on the this Nafion-Pt system of this study should also be minimal.

4. Conclusions

While the impregnation of 30 wt% Nafion on Pt/C had dramatic effects on the physical characteristics of Pt/C, such as the reduction of BET surface area from 170 m^2 g cat^{-1} to 37 m^2 g cat^{-1}, the overall effect of the Nafion on the adsorption capabilities of Pt for hydrogen and CO were minimal, based on both static chemisorption and in-situ surface hydrogen concentration results. Likewise, the similar rates of H_2–D_2 exchange for Pt/C and Nfn-Pt/C poisoned with ppm CO suggests that the effect of Nafion on the poisoning behavior of CO on the reaction is also minimal. However, for cyclopropane, a molecule larger than CO, a clear decrease in the rate of hydrogenolysis was observed in going from Pt/C to Nfn-Pt/C. While this decrease might be thought to be attributable to the blocking of Pt surface atoms by Nafion, due to the lack of evidence suggesting such an interaction exists from static chemisorption, H_2–D_2 exchange and hydrogen surface concentration results, the decrease in reaction rate is most likely due to internal diffusion limitations caused by the Nafion. Results from the modeling of a membrane (the Nafion in this case) over an idealized cylindrical pore show the effect of decreasing the size of the membrane opening, while keeping the pore diameter constant, to effectively decrease the value of E_a as a result of diffusion limitations through the membrane but not in the pore. In contrast, the similar values of E_a observed for H_2–D_2 exchange reaction on both Pt/C and Nfn-Pt/C suggests that the smaller effective pore openings in Nfn-Pt/C were not small enough to affect the smaller hydrogen molecules, as compared to cyclopropane. No blockage of Pt surface atoms by the Nafion via either physical and/or chemical interactions was observed. Based on all the measurements made, it appears that most of the Nafion is probably on the external surface of the carbon support, where it blocks micro pores significantly and partially blocks meso–macropores. Most of the Pt particles appear to reside in the meso–macropores.

Results from hydrogen surface concentration measurements on Pt/C and Nfn-Pt/C using H_2–D_2 exchange suggest a rapid diffusion of hydrogen and deuterium across the carbon surface at 80 °C. The increase in the amount of total exchangeable hydrogen going from Pt/C to Nfn-Pt/C was confirmed to be from the protonated sulfonic sites in the Nafion. It should be noted that while contact between the polymer and Pt particles is not required for proton transport, recent results from a new evaluation method for the effectiveness of Pt/C electrocatalysts clearly show the benefits of ionic contact in improving the apparent utilization of available Pt [44].

Acknowledgements

The authors would like to thank Dr. Douglas E. Hirt for the insightful discussions on the modeling portion of this paper and the Clemson Electron Microscope Facility for the help on acquiring the TEM images. This research was financially supported by the U.S. Department of Energy (Award No. DE-FG36-07GO17011).

References

[1] M.L. Perry, T.F. Fuller, J. Electrochem. Soc. 149 (2002) S59–S67.
[2] T. Li, A. Wlaschin, P.B. Balbuena, Ind. Eng. Chem. Res. 40 (2001) 4789–4800.
[3] R.B. Lin, S.M. Shih, J. Chin. Inst. Chem. Eng. 39 (2008) 475–481.
[4] R.M.Q. Mello, E.A. Ticianelli, Electrochim. Acta 42 (1997) 1031–1039.
[5] M. Watanabe, H. Igarashi, K. Yosioka, Electrochim. Acta 40 (1995) 329–334.
[6] M. Parthasarathy, V.K. Pillai, J. Chem. Sci. 121 (2009) 719–725.
[7] J.Z. Zhang, Z.M. Liu, J.G. Goodwin Jr., J. Power Sources 195 (2010) 3060–3068.

[8] E.B. Easton, T.D. Astill, S. Holdcroft, J. Electrochem. Soc. 152 (2005) A752–A758.
[9] G.C. Li, P.G. Pickup, J. Electrochem. Soc. 150 (2003) C745–C752.
[10] R.R. Passos, V.A. Paganin, E.A. Ticianelli, Electrochim. Acta 51 (2006) 5239–5245.
[11] M.G. Santarelli, M.F. Torchio, Energy Convers. Manage. 48 (2007) 40–51.
[12] K. Hongsirikarn, J.G. Goodwin Jr., S. Greenway, S. Creager, J. Power Sources 195 (2010) 30–38.
[13] R.A. Dalla Betta, J.A. Cusumano, J.H. Sinfelt, J. Catal. 19 (1970) 343.
[14] D.R. Kahn, E.E. Petersen, G.A. Somorjai, J. Catal. 34 (1974) 294–306.
[15] P.N. Ross, P. Stonehart, J. Res. Inst. Catal., Hokkaido Univ. 22 (1975) 22–41.
[16] R.L. Jia, C.Y. Wang, S.M. Wang, J. Mater. Sci. 41 (2006) 6881–6888.
[17] Z.H. Zhou, W.J. Zhou, S.L. Wang, G.X. Wang, L.H. Jiang, H.Q. Li, G.Q. Sun, Q. Xin, Catal. Today 93–95 (2004) 523–528.
[18] R.B. Anderson, J. Catal. 3 (1963) 50–56.
[19] E.P. Barrett, L.G. Joyner, P.P. Halenda, J. Am. Chem. Soc. 73 (1951) 373–380.
[20] K.J. Oberbroeckling, D.C. Dunwoody, S.D. Minteer, J. Leddy, Anal. Chem. 74 (2002) 4794–4799.
[21] S.L. Bernasek, G.A. Somorjai, J. Chem. Phys. 62 (1975) 3149–3161.
[22] P. Thostrup, E.K. Vestergaard, T. An, E. Laegsgaard, F. Besenbacher, J. Chem. Phys. 118 (2003) 3724–3730.
[23] N.Y. Chen, T.F. Degnan Jr., C.M. Smith, Molecular Transport and Reaction in Zeolites, John Wiley & Sons, Inc., 1994.
[24] M. Uchida, Y. Fukuoka, Y. Sugawara, N. Eda, A. Ohta, J. Electrochem. Soc. 143 (1996) 2245–2252.
[25] M. Montano, K. Bratlie, M. Salmeron, G.A. Somorjai, J. Am. Chem. Soc. 128 (2006) 13229–13234.
[26] M. Uchida, Y. Aoyama, N. Eda, A. Ohta, J. Electrochem. Soc. 142 (1995) 4143–4149.
[27] A.J. Robell, E.V. Ballou, M. Boudart, J. Phys. Chem. 63 (1964) 2748–2753.
[28] M. Andersen, M. Johansson, I. Chorkendorff, J. Phys. Chem. B 109 (2005) 10285–10290.
[29] J.C. Davies, R.M. Nielsen, L.B. Thomsen, I. Chorkendorff, A. Logadottir, Z. Lodziana, J.K. Norskov, W.X. Li, B. Hammer, S.R. Longwitz, J. Schnadt, E.K. Vestergaard, R.T. Vang, F. Besenbacher, Fuel Cells 4 (2004) 309–319.
[30] S.R. Longwitz, J. Schnadt, E.K. Vestergaard, R.T. Vang, E. Laegsgaard, I. Stensgaard, H. Brune, F. Besenbacher, J. Phys. Chem. B 108 (2004) 14497–14502.
[31] T.E. Hoost, J.G. Goodwin Jr., J. Catal. 130 (1991) 283–292.
[32] L.L. Hegedus, E.E. Petersen, J. Catal. 28 (1973) 150–156.
[33] R.D. Cortright, R.M. Watwe, B.E. Spiewak, J.A. Dumesic, Catal. Today 53 (1999) 395–406.
[34] G.A. Martin, R. Dutartre, S. Yuan, C. Marquez-Alvarez, C. Mirodatos, J. Catal. 177 (1998) 105–112.
[35] J. Schwank, J.Y. Lee, J.G. Goodwin Jr., J. Catal. 108 (1987) 495–500.
[36] G.R. Gallaher, J.G. Goodwin Jr., L. Guczi, Appl. Catal. 73 (1991) 1–15.
[37] S.D. Jackson, G.D. McLellan, G. Webb, L. Conyers, M.B.T. Keegan, S. Mather, S. Simpson, P.B. Wells, D.A. Whan, R. Whyman, J. Catal. 162 (1996) 10–19.
[38] M. Boudart, A. Aldag, J.E. Benson, N.A. Dougharty, C.G. Harkins, J. Catal. 6 (1966) 92.
[39] G.A. Somorjai, Abstr. Pap. Am. Chem. Soc. 189 (1985) 79.
[40] J.Z. Zhang, Y.T.Tsai, K.L. Sangkaewwattana, J.G. Goodwin Jr., J. Catal. 280 (2011) 89-95.
[41] F.Y.A. El-Kady, R. Mann, J. Catal. 69 (1981) 147–157.
[42] G.A. Truskey, F. Yuan, D.F. Katz, Transport Phenomena in Biological Systems, Pearson Education, Inc., Upper Saddle River, NJ, 2004.
[43] J.Z. Zhang, K. Hongsirikarn, J.G. Goodwin Jr., J. Power Sources 196 (2011) 6186-6195.
[44] M. Lee, M. Uchida, H. Yano, D.A. Tryk, H. Uchida, M. Watanabe, Electrochim. Acta 55 (2010) 8504–8512.
[45] F. Coloma, A. Sepulvedaescribano, F. Rodriguezreinoso, J. Catal. 154 (1995) 299–305.